

Supporting Information

# **Electrochemical Ammonia synthesis from dilute gaseous Nitric Oxide Reduction at Ambient Conditions**

*Haroon Ur Rasheed*<sup>1,2</sup>, *Jae Hyung Kim*<sup>1</sup>, *Taek-Seung Kim*<sup>1</sup>, *Kyungho Lee*<sup>1</sup>, *Joonmok Shim*<sup>1</sup>,

*Sung Hyung Kim*<sup>1</sup> and *Hyung Chul Yoon*<sup>1,\*</sup>

<sup>1</sup> Clean Fuel Research Laboratory, Korea Institute of Energy Research (KIER), 152 Gajeong-ro, Yuseong-gu, Daejeon 34129, Republic of Korea

<sup>2</sup> Department of Clean Energy Engineering, Korea National University of Science and Technology (UST), 217, Gajeong-ro, Yuseong-gu, Daejeon 34113, Republic of Korea

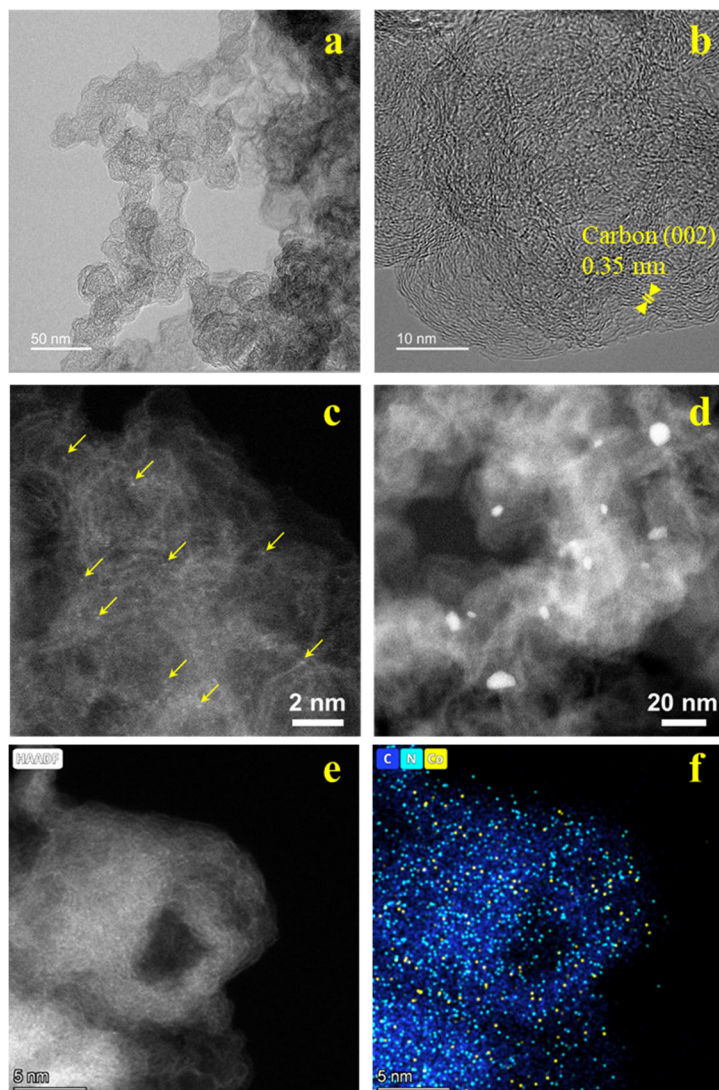


Figure S1. Structural characterization of Co-NC: (a) Low magnification FE-TEM image, (b) HR-TEM image, (c-e) STEM images, and (f) EDS elemental mapping, respectively.

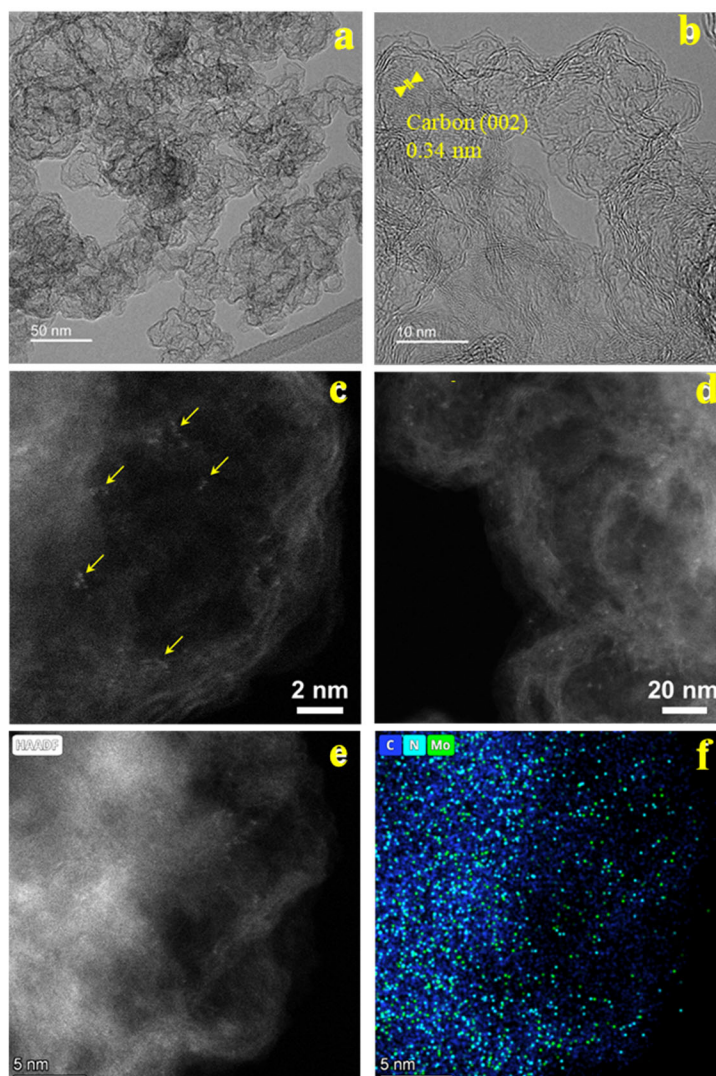


Figure S2. Structural characterization of Mo-NC: (a) Low magnification FE-TEM image, (b) HR-TEM image, (c-e) STEM images, and (f) EDS elemental mapping, respectively.

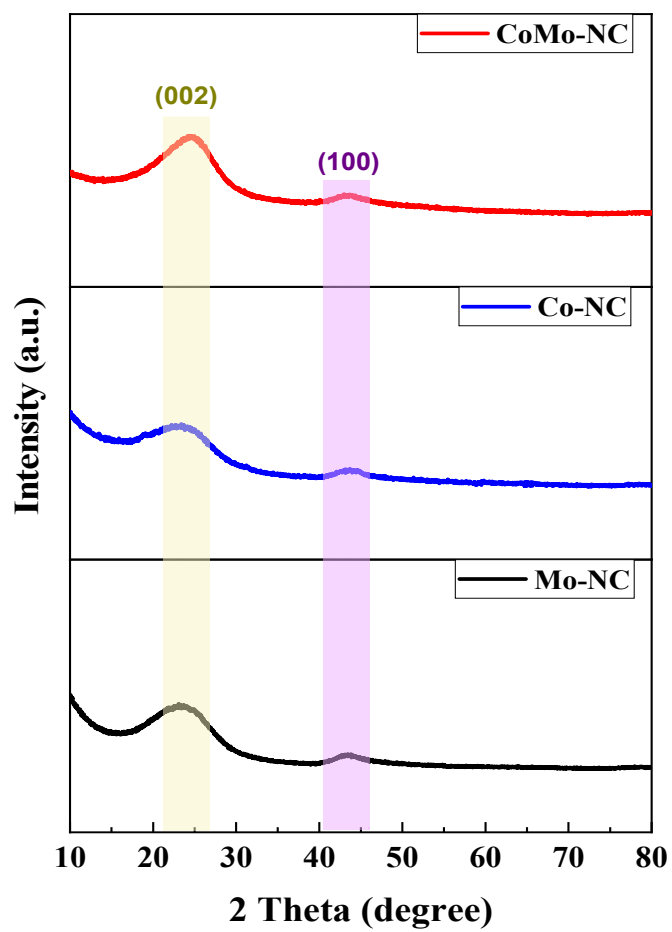


Figure S3. XRD patterns of Mo-NC, Co-NC, and CoMo-NC (Bottom to top).

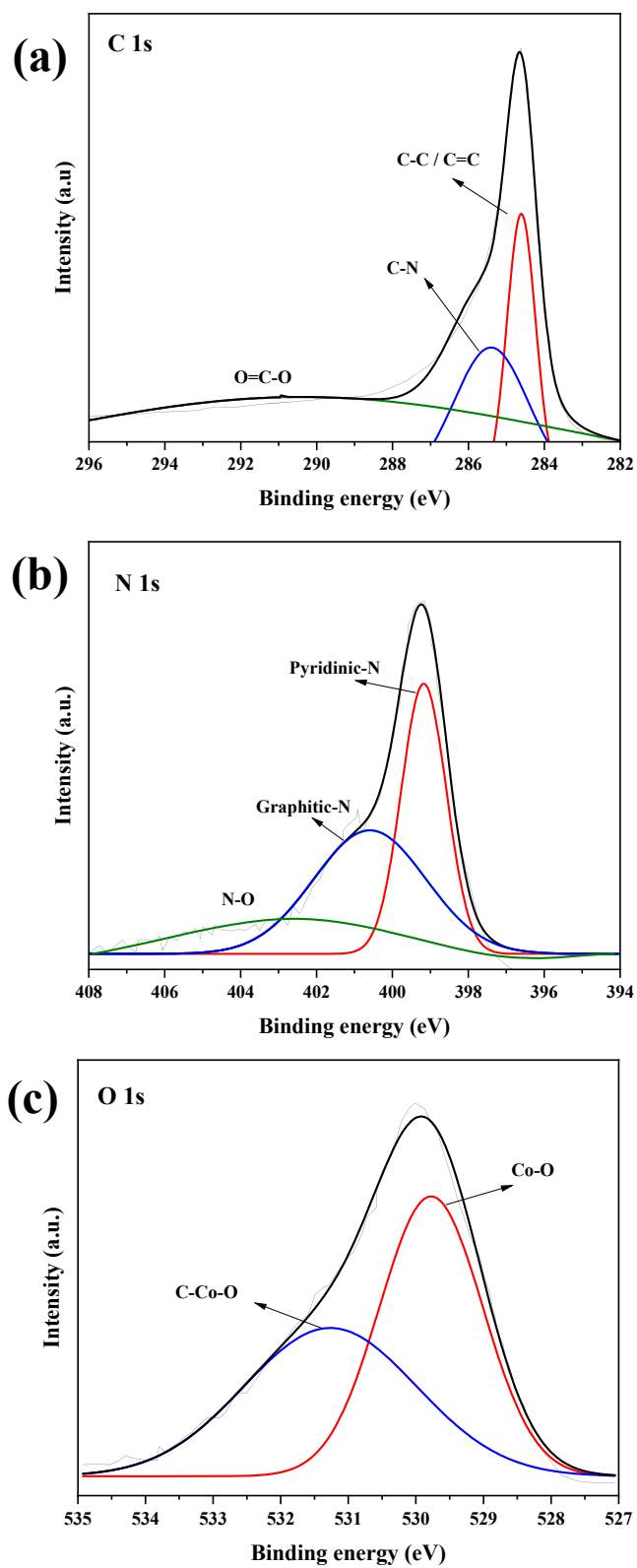


Figure S4. High-resolution XPS spectra of Co-NC: (a) Carbon (C 1s), (b) Nitrogen (N 1s), and (c) Oxygen (O 1s).

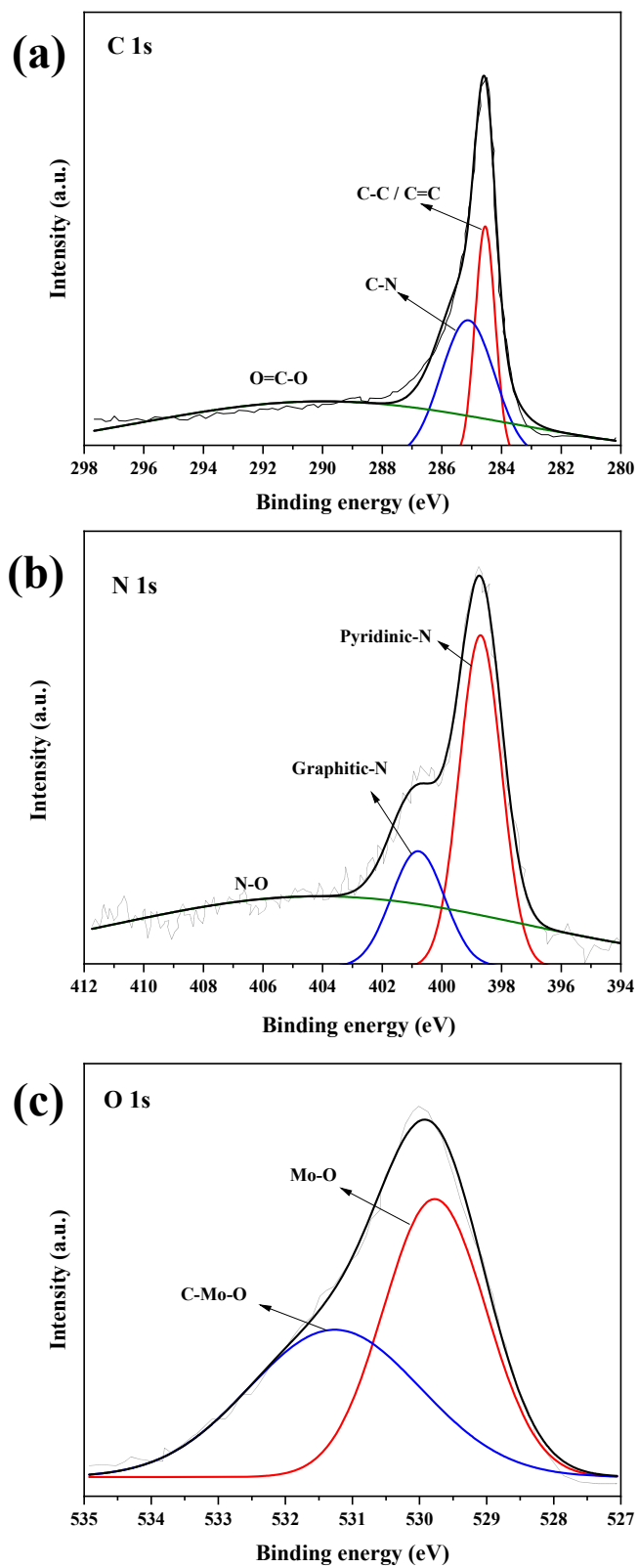


Figure S5. High-resolution XPS spectra of Mo-NC: (a) Carbon (C 1s), (b) Nitrogen (N 1s), and (c) Oxygen (O 1s).

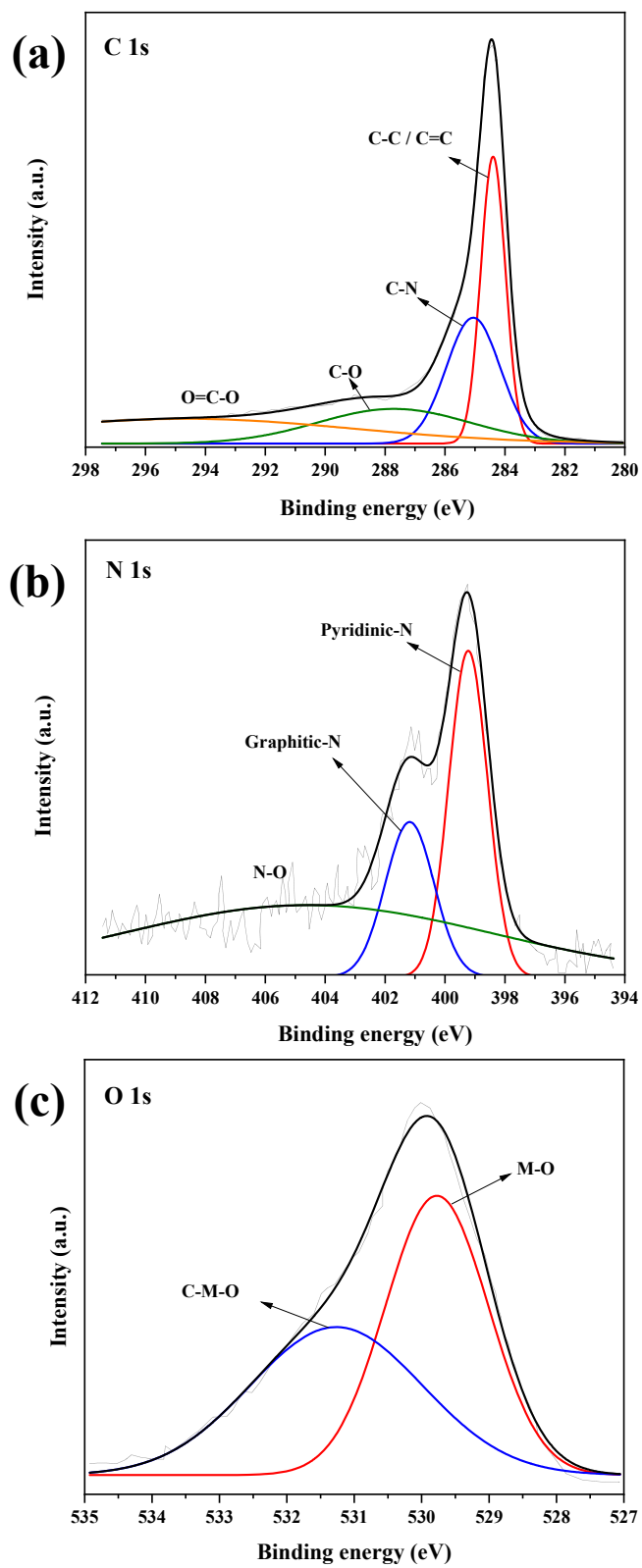


Figure S6. High-resolution XPS spectra of CoMo-NC: (a) Carbon (C 1s), (b) Nitrogen (N 1s), and (c) Oxygen (O 1s).

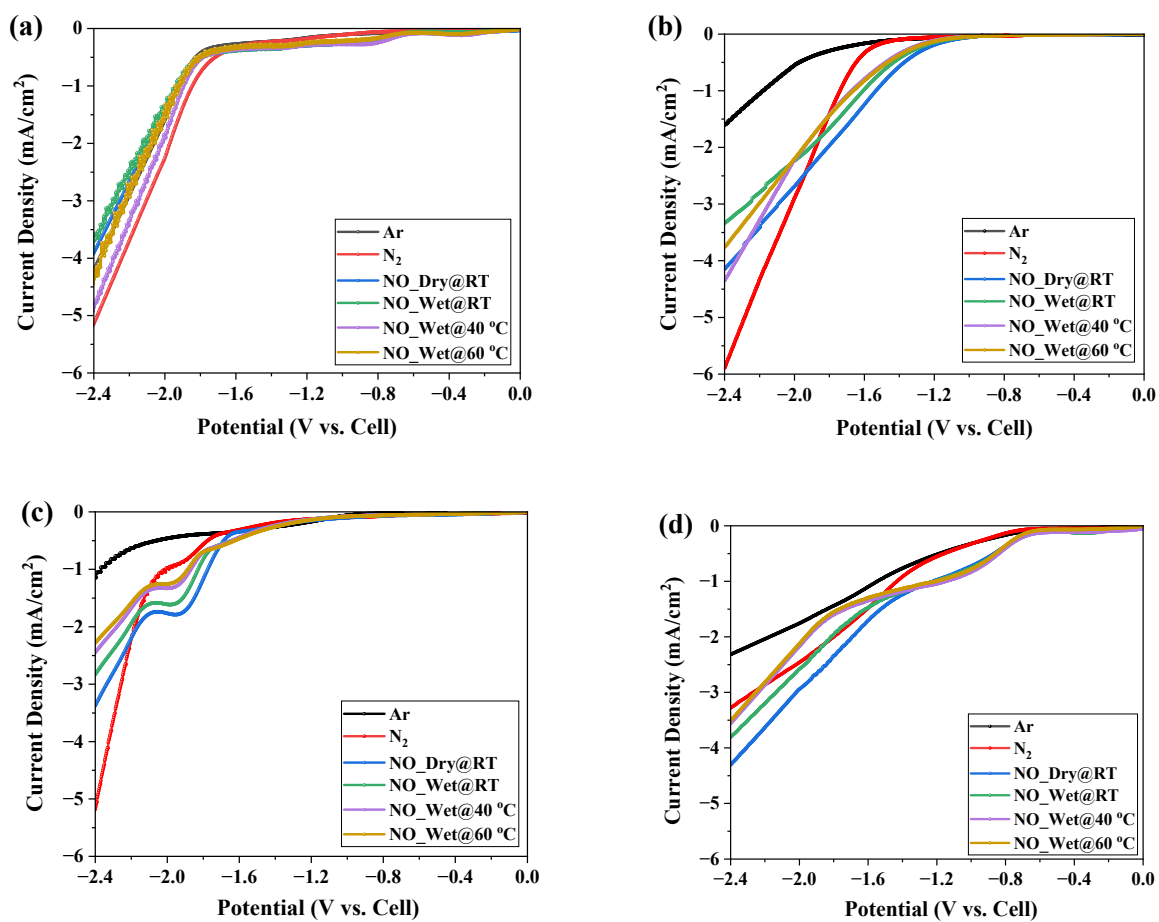


Figure S7. LSV tests of electrocatalysts: (a) Co-VC, (b) Co-NC, (c) Mo-NC, and (d) CoMo-NC at a scan rate of 10 mV s<sup>-1</sup>.

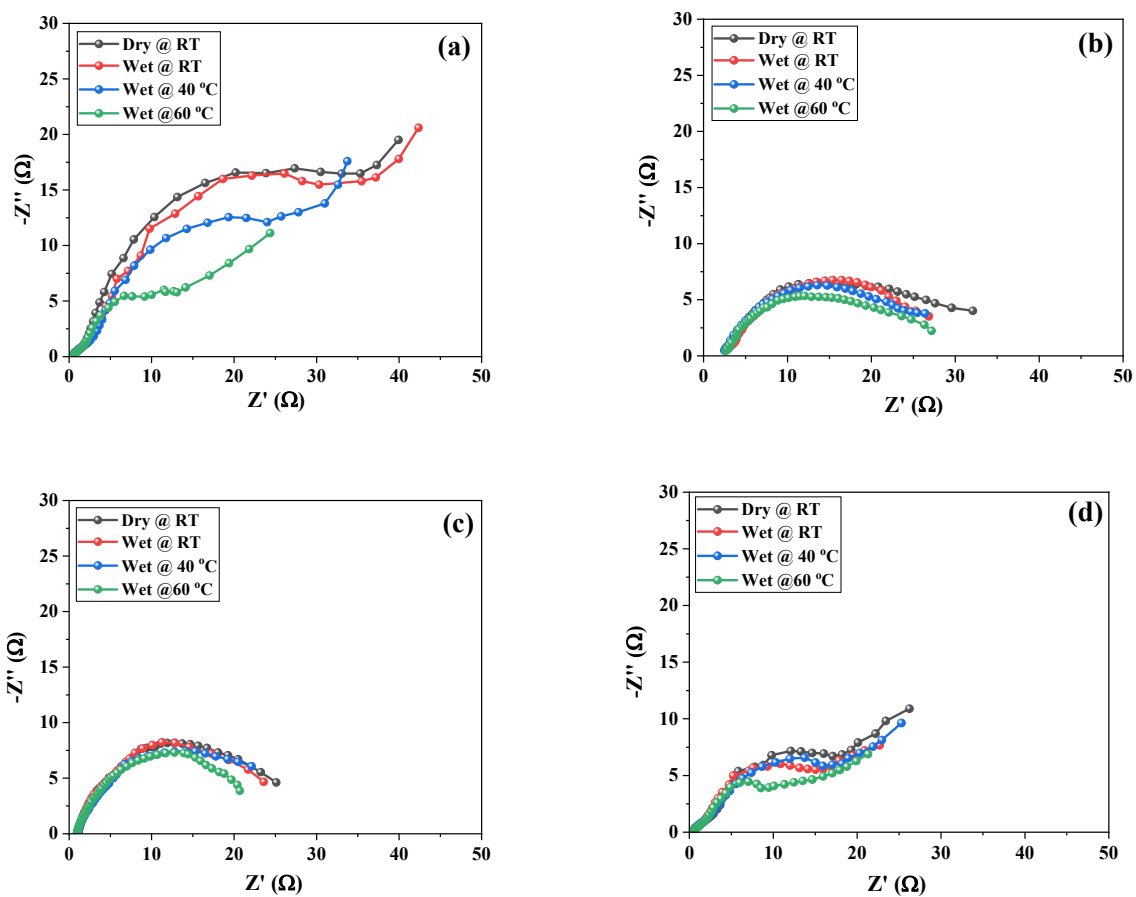


Figure S8. Electrochemical impedance spectroscopy (EIS) measurement in the range of 100 kHz to 100 mHz under potentiostatic mode at (a) -1.6, (b) -1.8, (c) -2.0, and (d) -2.2 V<sub>cell</sub> at excitation amplitude of 20 mV for Co-VC.

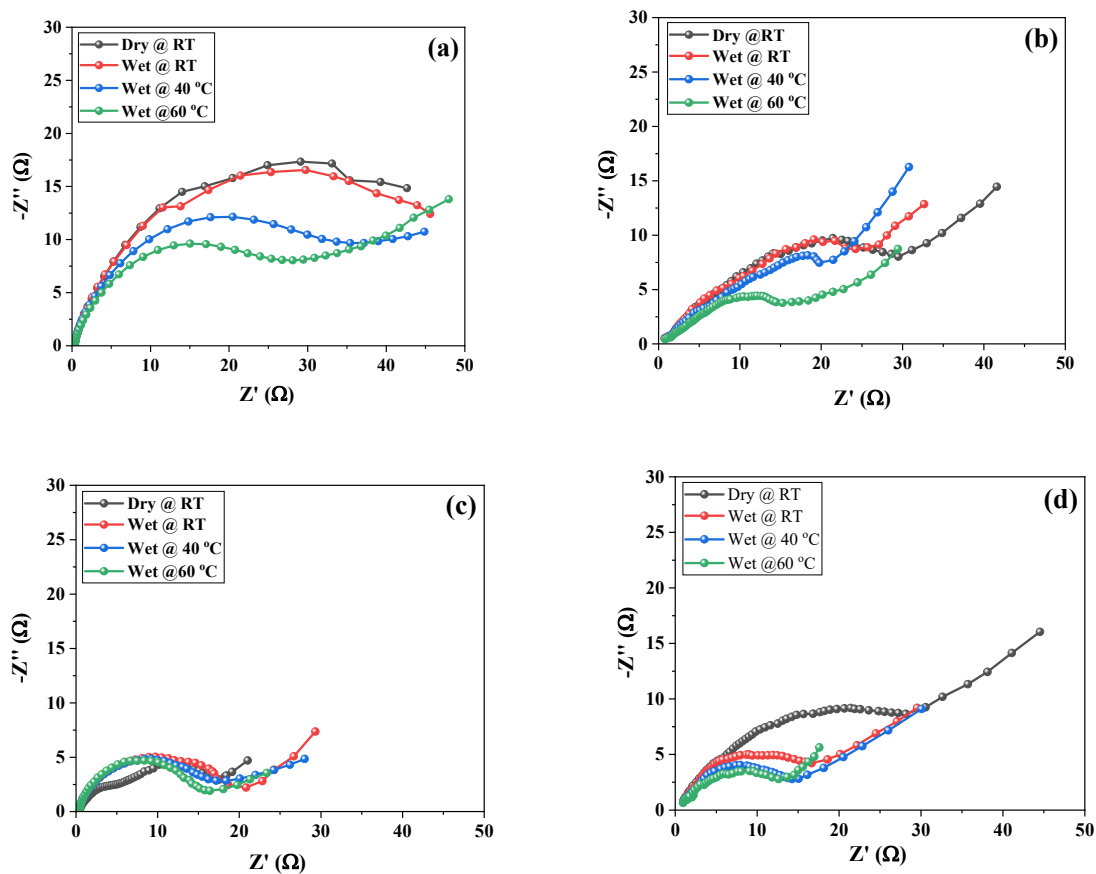


Figure S9. Electrochemical impedance spectroscopy (EIS) measurement in the range of 100 kHz to 100 MHz under potentiostatic mode at (a) -1.6, (b) -1.8, (c) -2.0, and (d) -2.2 V<sub>cell</sub> at excitation amplitude of 20 mV for Co-NC.

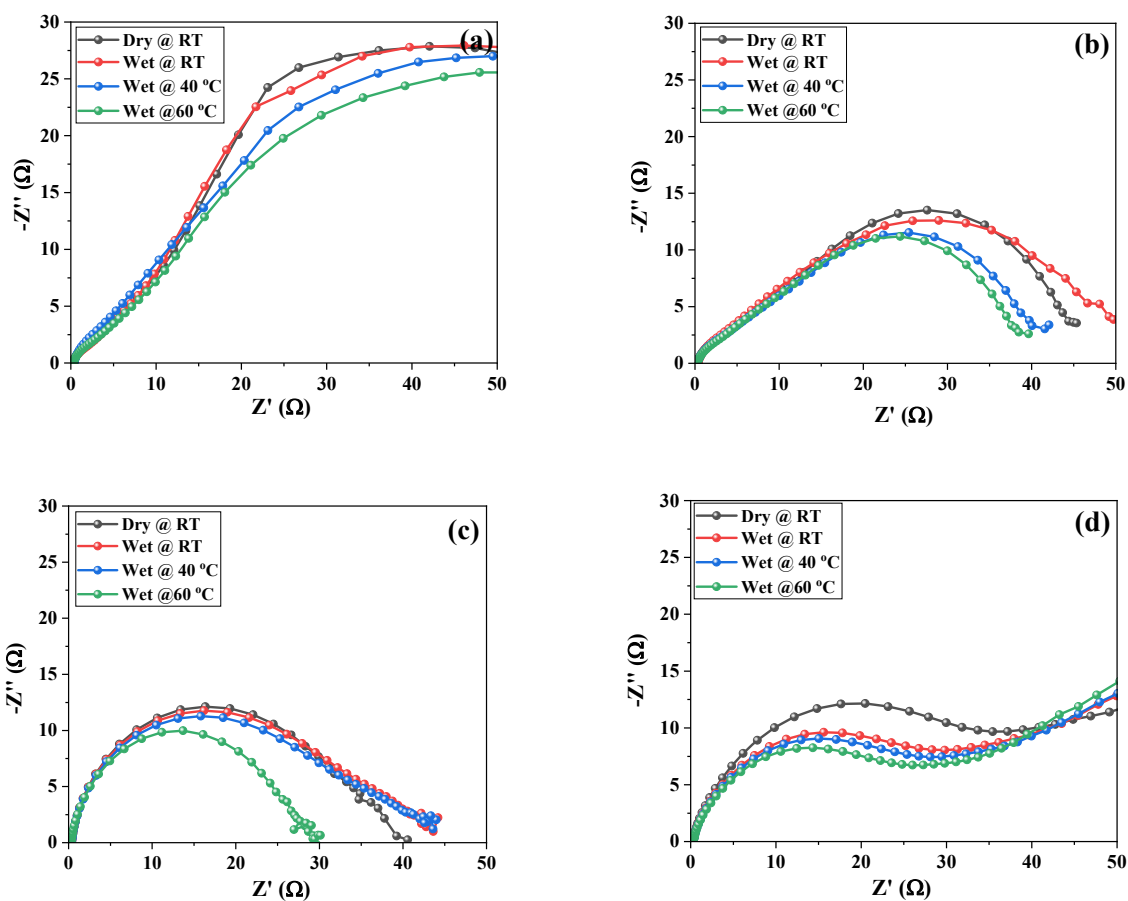


Figure S10. Electrochemical impedance spectroscopy (EIS) measurement in the range of 100 kHz to 100 mHz under potentiostatic mode at (a) -1.6, (b) -1.8, (c) -2.0, and (d) -2.2 V<sub>cell</sub> at excitation amplitude of 20 mV for Mo-NC.

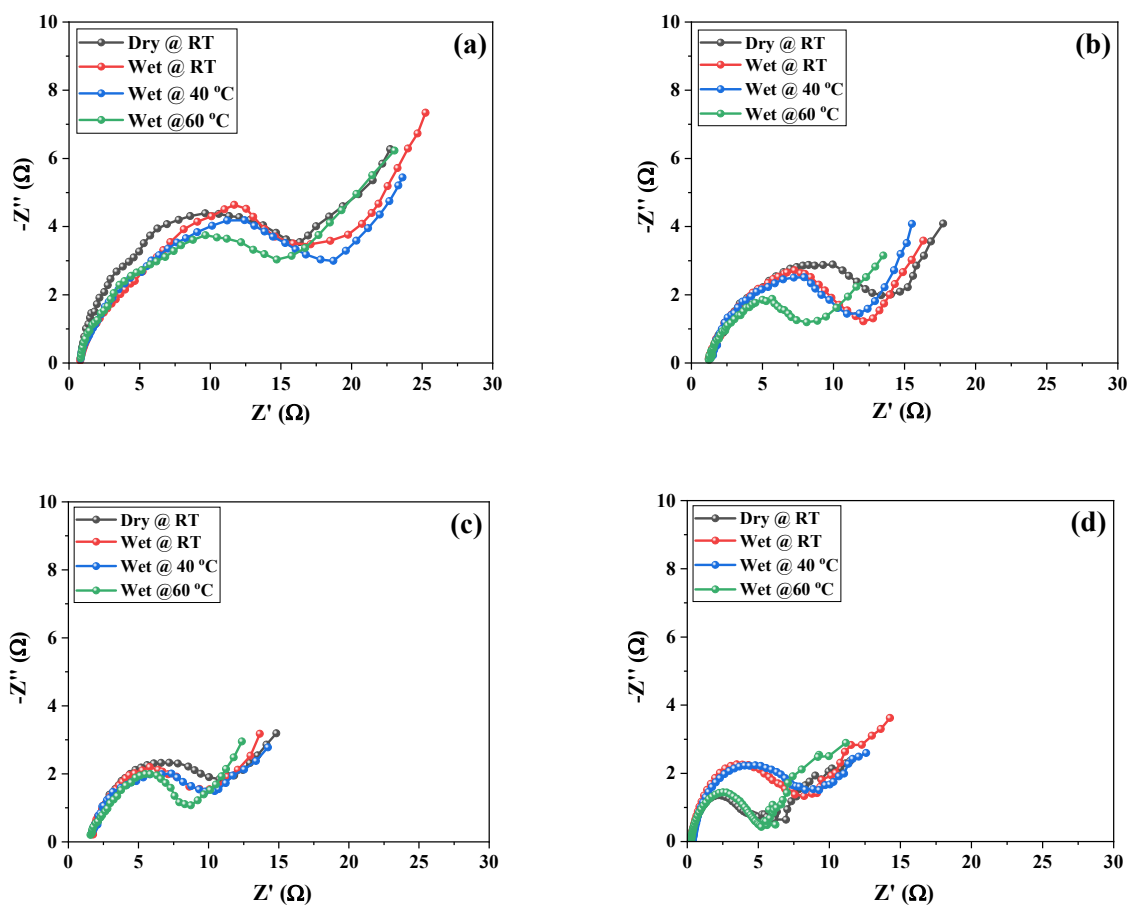


Figure S11. Electrochemical impedance spectroscopy (EIS) measurement in the range of 100 kHz to 100 mHz under potentiostatic mode at (a) -1.6, (b) -1.8, (c) -2.0, and (d) -2.2 V<sub>cell</sub> at excitation amplitude of 20 mV for CoMo-NC.

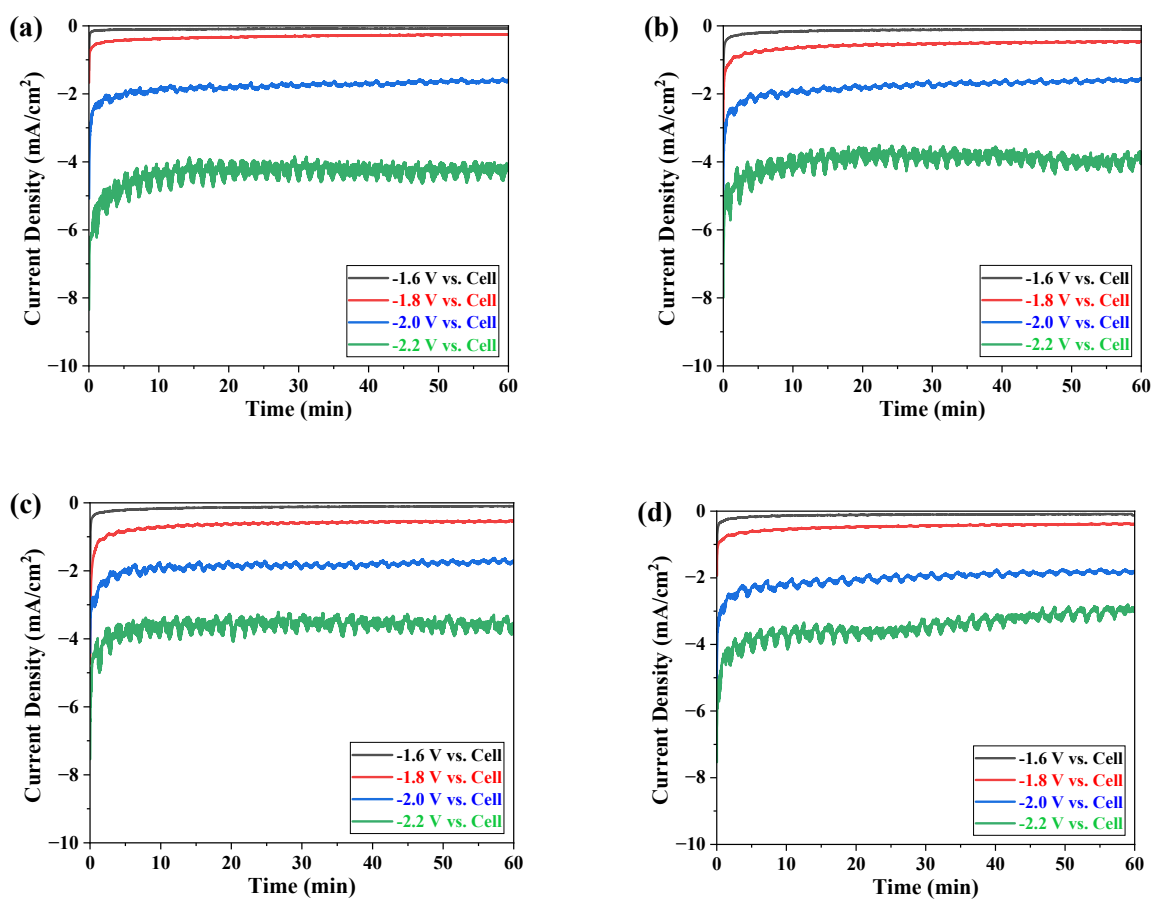


Figure S12. Chronoamperometry tests of Co-VC at a constant potential (vs. cell) for 1 h with (a) Dry@RT NO, (b) Wet@RT, (c) Wet@40 °C, and (d) Wet@60 °C condition.

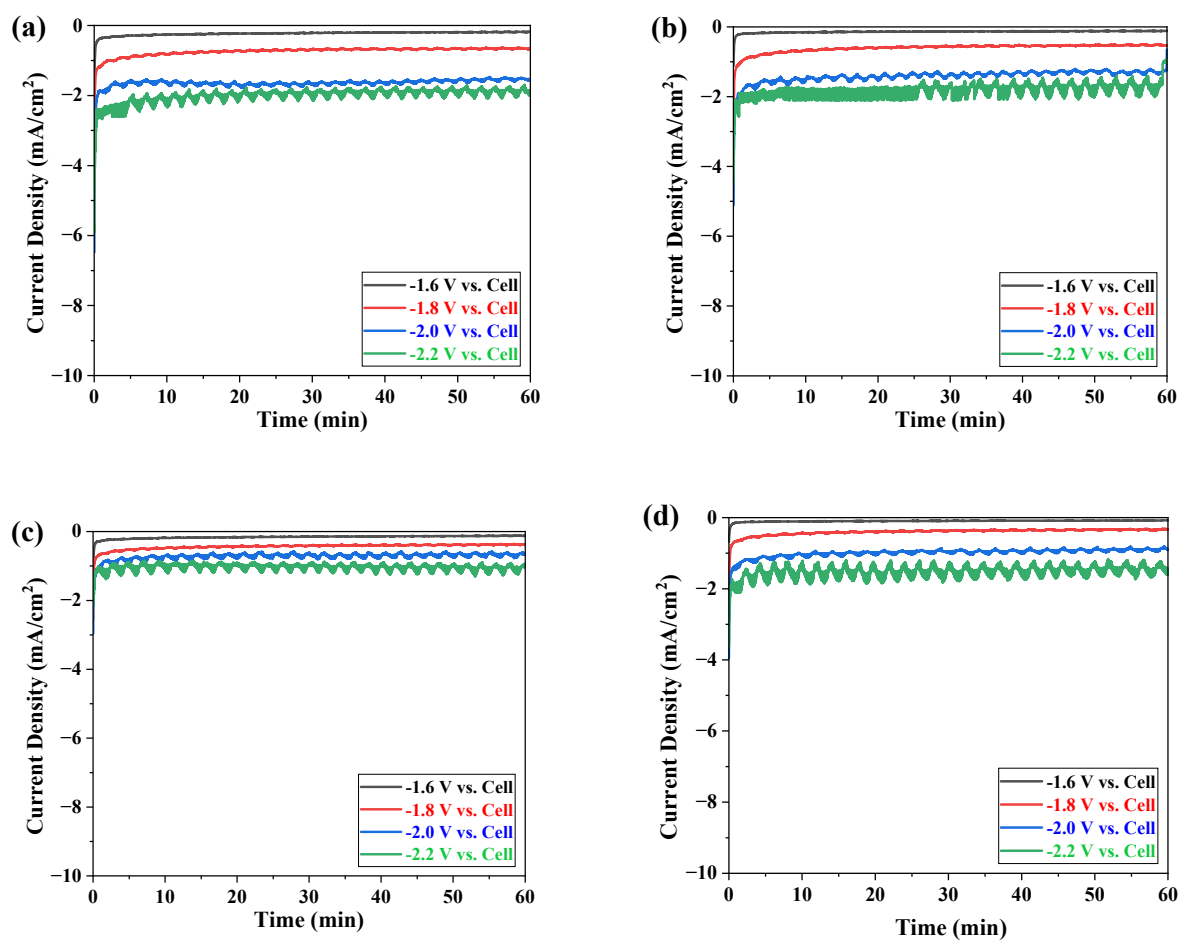


Figure S13. Chronoamperometry tests of Co-NC at a constant potential (vs. cell) for 1 h with (a) Dry@RT NO, (b) Wet@RT, (c) Wet@40 °C, and (d) Wet@60 °C condition.

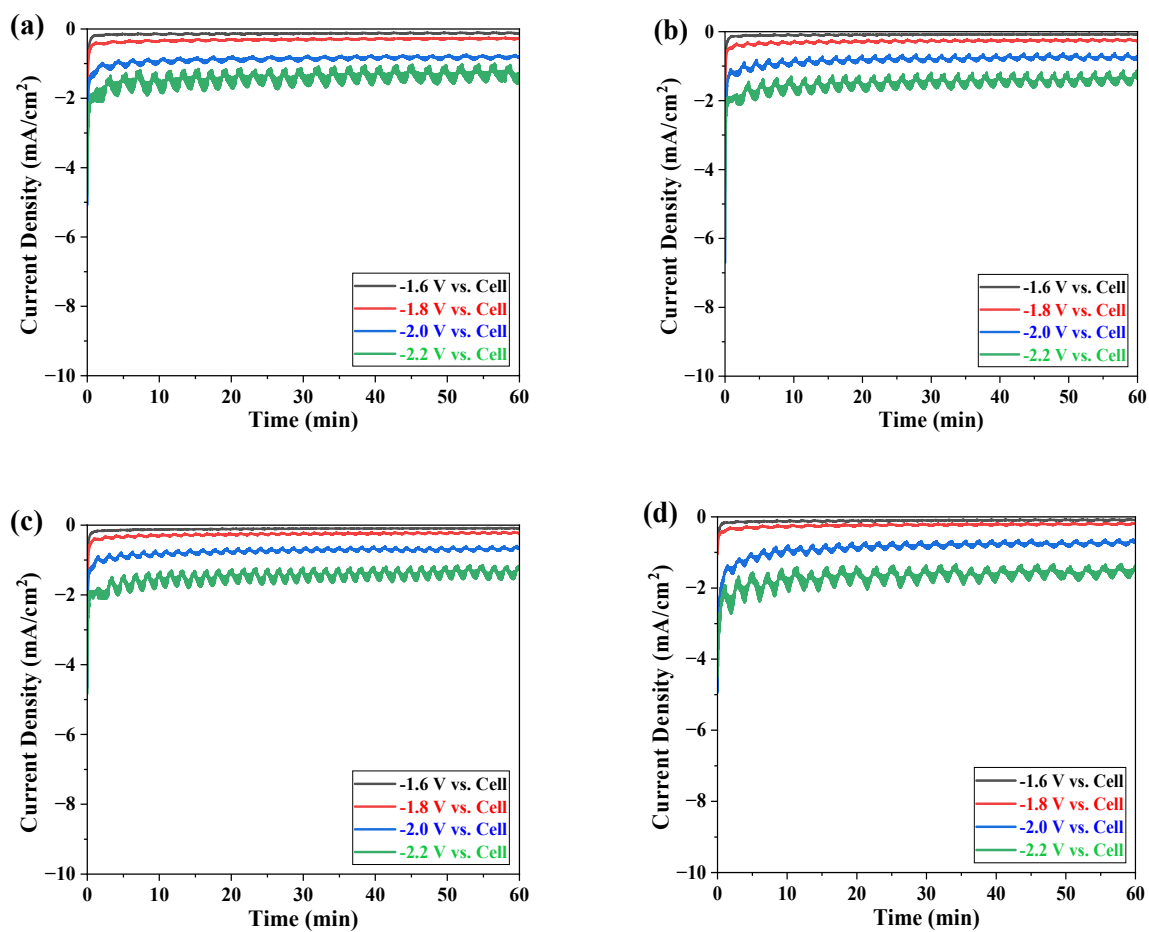


Figure S14. Chronoamperometry tests of Mo-NC at a constant potential (vs. cell) for 1 h with (a) Dry@RT NO, (b) Wet@RT, (c) Wet@40 °C, and (d) Wet@60 °C condition.

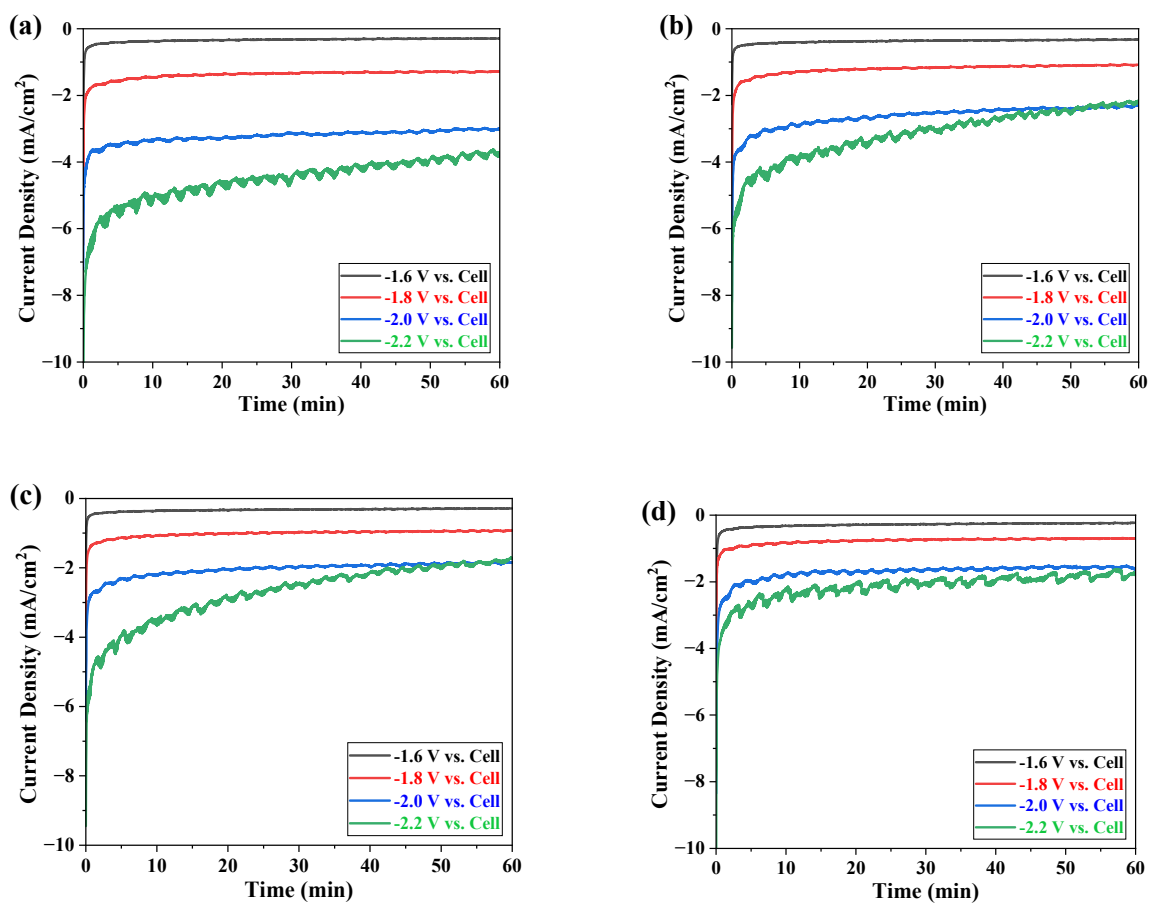
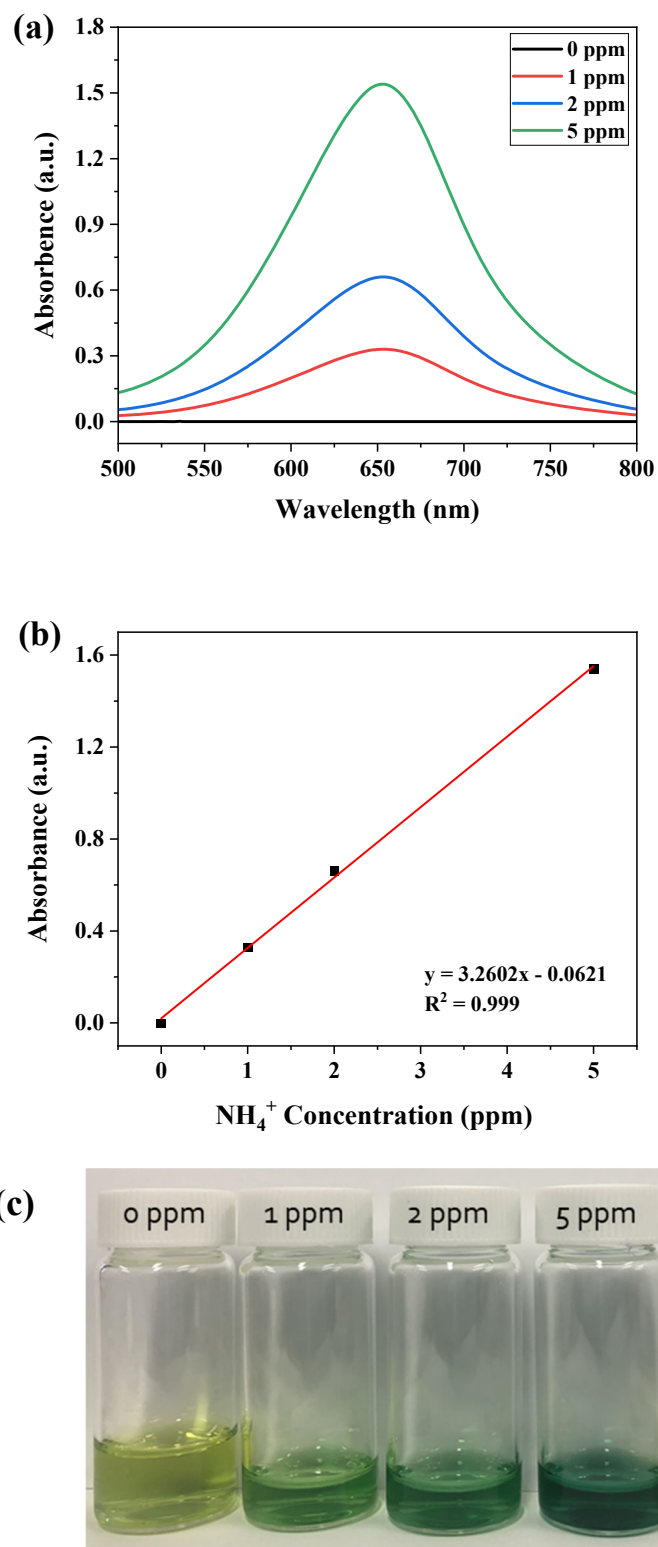


Figure S15. Chronoamperometry tests of CoMo-NC at a constant potential (vs. cell) for 1 h with (a) Dry@RT NO, (b) Wet@RT, (c) Wet@40 °C, and (d) Wet@60 °C condition.



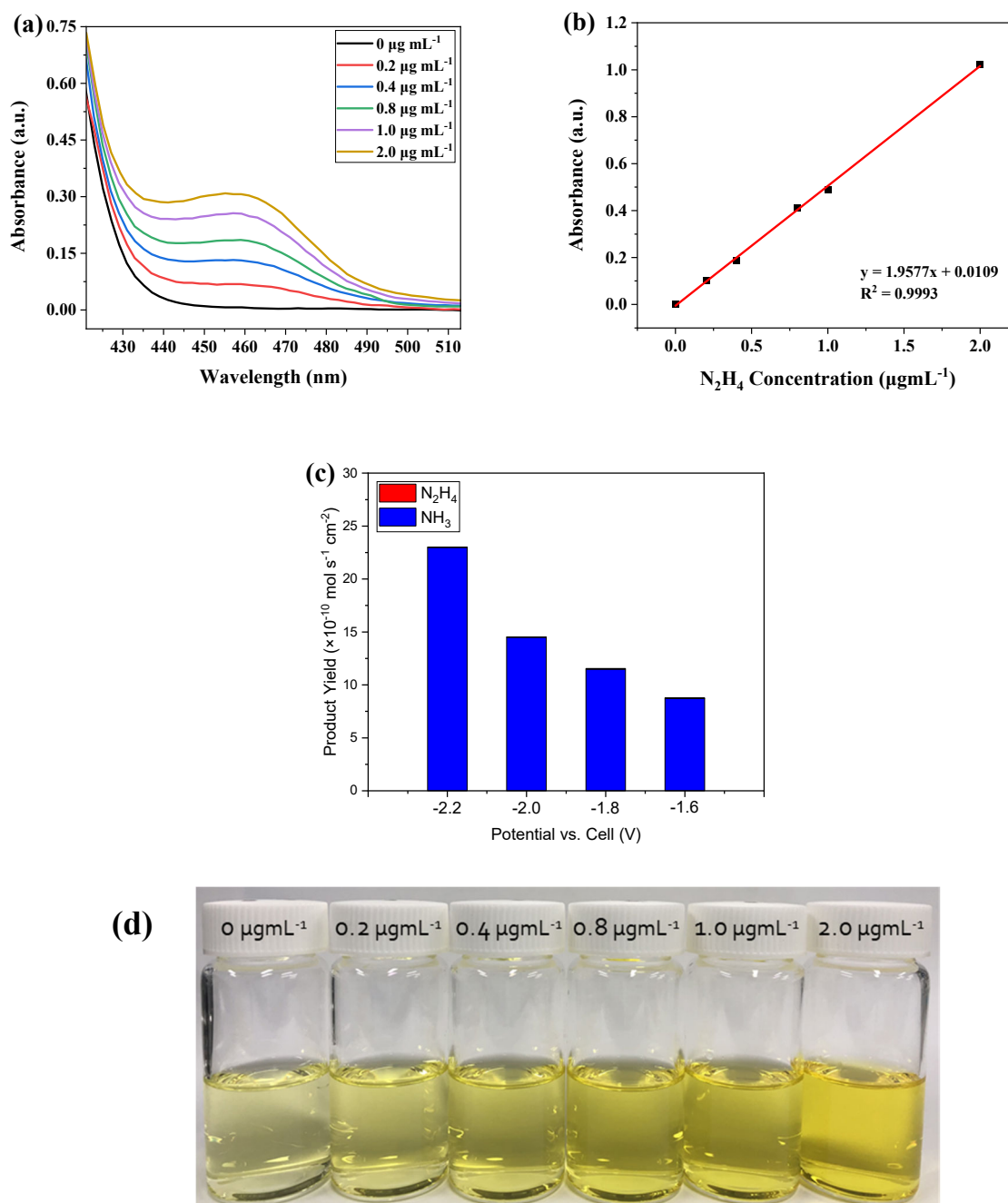


Figure S17. (a) UV-vis spectra (b) calibration curve, (c)  $\text{NH}_3$  and  $\text{N}_2\text{H}_4$  yield rates in NORR at different potentials, and (d) photograph of standard  $\text{N}_2\text{H}_4$  solutions.

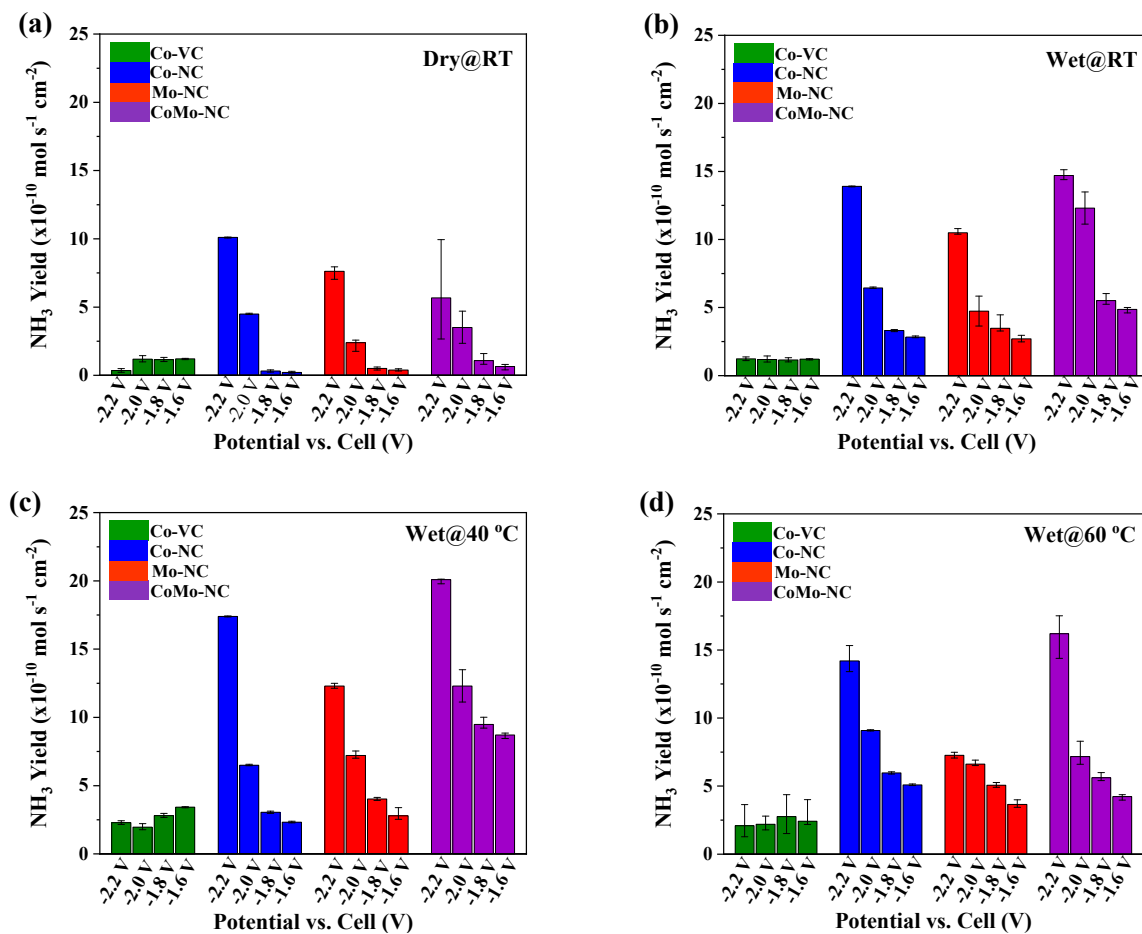


Figure S18.  $\text{NH}_3$  yield rates at different potentials (vs. cell) and NO feed of (a) Dry@RT, (b) Wet@RT, (c) Wet@40 °C, and (d) Wet@60 °C of Co-VC, Co-NC, Mo-NC, and CoMo-NC.

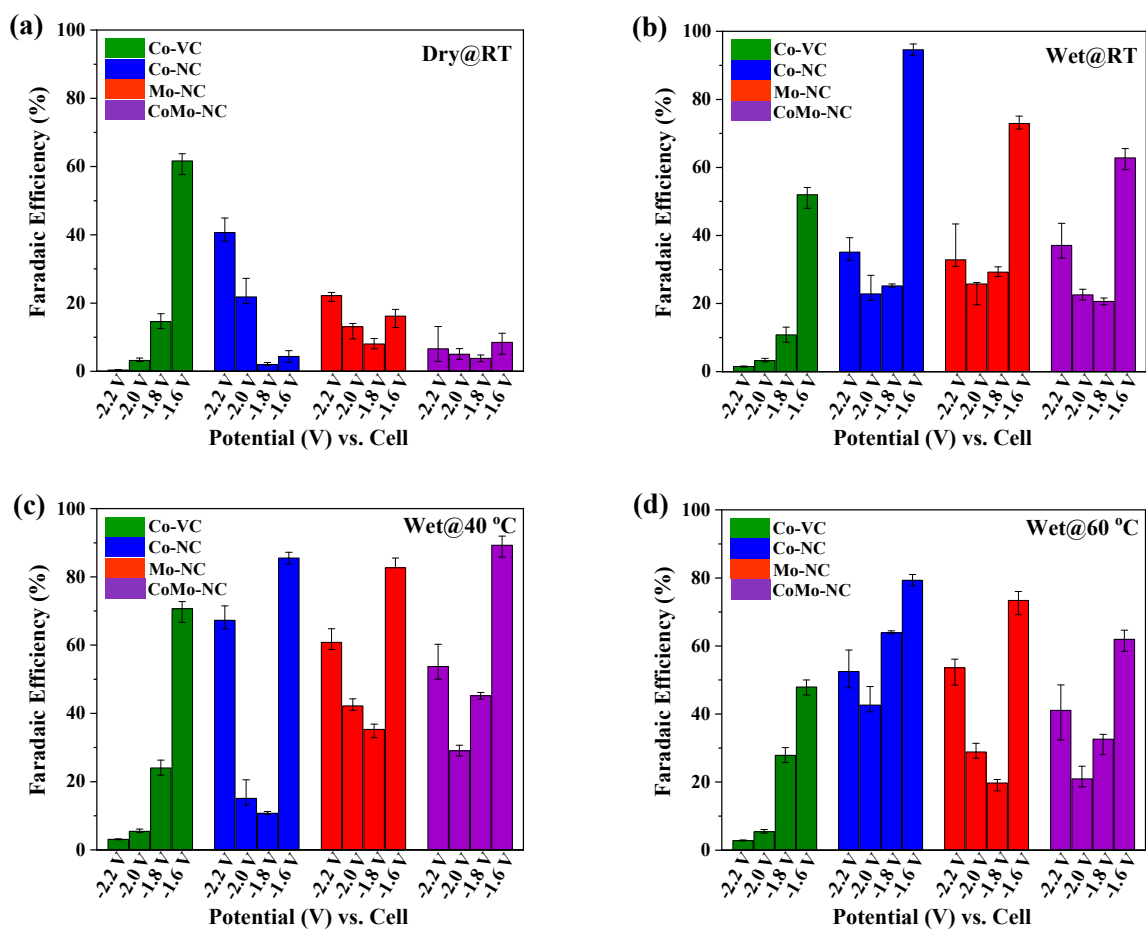


Figure S19. Faradaic efficiencies at different potentials (vs. cell) and NO feed of (a) Dry@RT, (b) Wet@RT, (c) Wet@40 °C, and (d) Wet@60 °C of Co-VC, Co-NC, Mo-NC, and CoMo-NC.

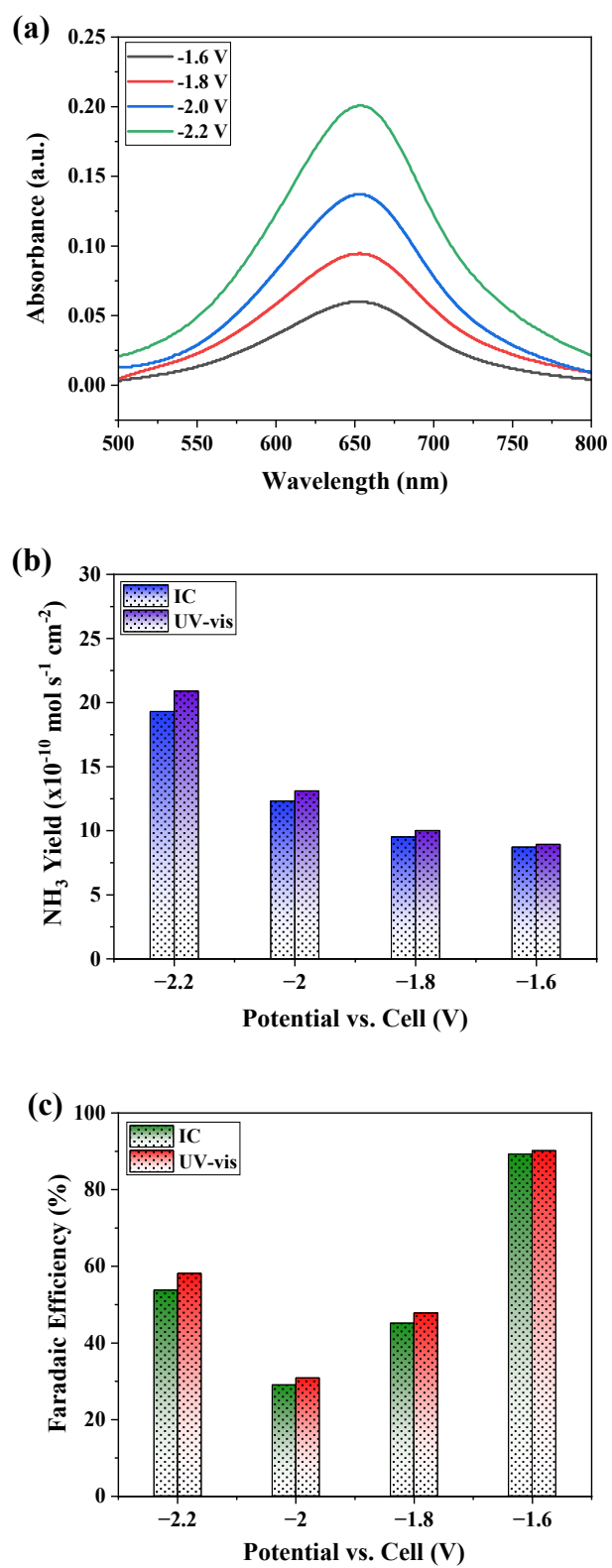


Figure S20. (a)  $\text{NH}_3$  yield rates and (b)  $\text{FE}_{\text{NH}_3}$  quantified by IC and UV-vis (c) UV-vis absorption spectra at different potentials after 1 h electrolysis for  $\text{NH}_3$  quantification.

Table S1. CoMo-C comparison with reported electrocatalysts for electrochemical ammonia synthesis

Reactant Gas	Electrocatalysts	Electrolyte	Cell Type	NH <sub>3</sub> Yield Rate (μmol h <sup>-1</sup> cm <sup>-2</sup> )	FE <sub>NH<sub>3</sub></sub> (%)	Ref
Pure NO	Cu foam	0.25 M Li <sub>2</sub> SO <sub>4</sub>	H-type	517.1	93.5	[4]
10% NO	K <sub>2</sub> [Ni(CN) <sub>4</sub> ]	Catholyte-free	Flow type	1128.9	89.5	[6]
1% NO	Ag Nanoparticles	FeEDTA+ 0.5 M PBS	Flow type	360	100	[13]
10% NO	Fe/C	0.5 M PBS	Flow type with GDE	908	77	[25]
10% NO	Fe/C	0.5 M H <sub>2</sub> SO <sub>4</sub>	Flow type with GDE	1239	50.4	[25]
N <sub>2</sub>	Fe/CNT	Catholyte-free	H-type with GDE	0.013	0.05	[33]
N <sub>2</sub>	N-doped carbon nanopikes	0.25 M LiClO <sub>4</sub>	H-type	5.7	11.6	[34]
4.8% NO	Ru/C	Catholyte-free	Flow type	510	93	[35]
99.9% NO	Cu <sub>75</sub> Ni <sub>25</sub> @NC	1 M KOH	H-type	3.6	79	[36]
Pure NO	CuRh NSs	0.1 M Na <sub>2</sub> SO <sub>4</sub>	H-type	436	93.1	[37]
<b>1% NO</b>	<b>CoMo-NC</b>	<b>Catholyte-free</b>	<b>Flow type</b>	<b>8.34</b>	<b>94.6</b>	<b>This work</b>